Research Article | Vol. 10, No. 3 | 1 Mar 2019 | BIOMEDICAL OPTICS EXPRESS 1136
Biomedical Optics EXPRESS

3,3′-thiodipropanol as a versatile refractive index-matching mounting medium for fluorescence microscopy

Milvia Iris Alata Tejedo,[1] Juan Carlos Martínez Cervantes,[1] Adrian Saul Jimenez Roldán,[2] Mario Rodriguez,[1] Arturo González Vega,[2] and Valeria Piazza[1,*]

[1]*Centro de Investigaciones en Óptica, Loma Del Bosque 115, León C.P. 37150, Mexico*
[2]*Depto. de Ingenierías Química, Electrónica y Biomédica, DCI, Universidad de Guanajuato, Loma del Bosque 103, León, Mexico*
**vpiazza@cio.mx*

Abstract: High resolution fluorescence microscopy requires optimization of the protocols for biological sample preparation. The optical and chemical characteristics of mounting media are among the things that could be modified to achieve optimal image formation. In our search for chemical substances that could perform as mounting media, 3,3′-thiodipropanol (TDP) emerged as a sulfide with potentially interesting characteristics. In this work, several tests of its performance as a mounting medium for fluorescence microscopy of biological samples were performed, including the labeling of filamentous actin with fluorescent phalloidins. The refractive index dispersion curve of pH-adjusted TDP was experimentally obtained in the visible range and compared to the dispersion curves of commercial and lab-made mounting media. The effects on the fluorescence of commonly used dyes were tested by using TDP as a solvent and measuring the relative fluorescence quantum yield of the dyes. By being able to mix TDP in any concentration with water and 2,2′-thiodiethanol (TDE), it was possible not only to fine-tune the refractive index of the resulting solution, but also to preserve the compatibility of TDP with the most popular and efficient fluorescent actin staining used in biological microscopy.

1. Introduction

Use of high numerical aperture lenses, low background staining protocols, high quality glass for slide preparation are common steps that can be undertaken to improve the quality of the fluorescence images that could be generated from biological microscopy slides. Another aspect that needs to be considered in the staining and mounting protocol is the chemical substance that is used to seal the sample between the slide and the coverslip. Such material, called mounting medium, needs to fulfil some requirements.

First of all, it should be a colorless and transparent liquid, capable of permeating into cells and tissues and not causing any dye diffusion or fading. In addition to the lack of adverse effect on tissue components, it is desirable for the mounting medium to be harmless for the user. Another often disregarded characteristic is the refractive index (n) of the mounting medium, which for high resolution, diffraction-limited microscopy should be as close as possible to that of glass and immersion oil, i.e., 1.515 (by convention measured at the sodium spectral line). When resolution is not an issue and/or the limiting factor is the type of lens available, another useful characteristic is that the same medium could be diluted to vary its refractive index, to match the n of water or glycerol, other common options for liquid immersion objectives. The maximal homogeneity in n at the two coverslip boundaries is required to avoid size scaling in the z axis, reduction of the effective numerical aperture and reduction in resolution and peak intensity [1].

#351460 https://doi.org/10.1364/BOE.10.001136
Journal © 2019 Received 8 Nov 2018; revised 7 Jan 2019; accepted 11 Jan 2019; published 11 Feb 2019

Biomedical Optics EXPRESS

In a search among different simple compounds, TDP has emerged as an interesting candidate for mounting medium: it is liquid, colorless, possesses a high *n* when undiluted, it is miscible in water, non-toxic and its potential use as a mounting medium would represent a cheaper alternative compared to other commercial products. In this work, a thorough optical characterization of TDP was performed and the chemical was tested for its use as mounting medium for biological samples stained with common used fluorophores. The fluorescent slides were subsequently imaged with confocal microscopy, confirming its suitability for this application.

The major improvement that comes with the use of TDP as mounting medium is its compatibility with the use of toxin-based actin markers, in particular phalloidin. Differently from what happens with the related molecule TDE, phalloidin staining of microfilaments maintains its morphology and fluorescent properties after mounting in TDP. Additionally, TDP and TDE can be mixed, to finely adjust the *n* of the medium for high resolution fluorescent microscopy without losing the capability of staining actin with phalloidin. This type of actin decoration is by far the most popular in biomedical microscopy experiments, both for staining and counterstaining, due to the simplicity of the protocol and the quality of the outcome. For this reason, widening the application range of sulfides mounting to actin staining will add an important tool to high resolution biological fluorescent microscopy protocols.

2. Methods and materials

2.1 Mounting media and immersion oil

2,2′-thiodiethanol (TDE) and 3,3′-thiodipropanol (TDP) (Sigma Aldrich No. 166782 and 205346 respectively) pH were adjusted to 7 ± 1 using sodium hydroxide. 1 mL of TDE is adjusted to the desired pH value using approx. 2 µL of 0.05M NaOH. In the case of TDP, 1 mL is adjusted using 12.5 µL of 0.25M NaOH, although the volumes could vary depending on the lot number. The terms aTDE and aTDP refer to the media prepared as above. TDE and TDP are viscous compounds and provide inconsistent readings with the electrodes normally used for pH measurement, therefore pH indicator strips (Macherey Nageland) and the pH indicator phenol red (No. P4758, Sigma Aldrich) were also used.

VectaShield (abbreviated as VS, Vector Labs, Product number H 1000), ProLong Diamond (abbreviated as PLD, Thermo Fisher Scientific, No P36965), Dako (DAKO North America Inc., S3023) and Immersol 518-F (Zeiss Item Number: 444960-0000-000) were also used in this work.

2.2 Refractive index

The refractive index of mounting media was measured using an Abbe refractometer Type-WY1A (Edmund Optics, Barrington, U.S.A.). The n_D value refers to refractive index measured at 589 nm obtained using a white light source directed to the illumination window of the refractometer and using the compensating prism to deflect other wavelengths.

2.3 Dispersion measurements

Two different types of light sources were used to cover the visible range from 410 to 680 nm: a SCT500 supercontinuum laser (FYLA, Spain) whose spectrum ranges from 500 to 2150 nm and 2 LED sources with spectra centered in 420 nm (thereafter called LED_{420}, FWHM: 18 nm) and 440 nm (LED_{440}, FWHM: 19 nm). LED_{420} was used for the 410 nm reading and LED_{440} for the 440 and 470 nm. Seven data points in the range of 500-680 nm were measured with the laser in wavelength steps of 30 nm. The 590 nm point was replaced with 589 nm since it approximates to the sodium line conventionally used for reporting refractive indices.

Through a double-convex lens (Edmund Optics, U.S.A), the light beam from the LEDs was focused to a DMC1-03 monochromator (Optometrics, USA). Data from the manufacturer

Biomedical Optics EXPRESS

indicates a resolution of 2.16 nm for a slit width of 300 μm. For the laser, no lens was required since an optic collimator is coupled to the fiber. Another double-convex lens was placed to expand the beam so that it could fill the illumination window of the Abbe refractometer. The refractometer is provided with a compensator dial to filter out the sodium D line and deflect other wavelengths. During the measurements, the compensator was set to position 30 to avoid wavelength-dependent beam deviation. A CCD cell phone camera focusing on the eyepiece of the refractometer was mounted on a mechanical support, allowing an instantaneous view of the eyepiece image to be seen on the cell phone screen. The whole system was placed in a temperature-controlled room at 21°+/– 0.5° C.

2.4 Curve fitting for dispersion data

The dispersion curve for the refractive index in the visible range was approximated using the least squares fitting method for a four terms Cauchy's dispersion equation:

$$n = A_0 + \frac{A_1}{\lambda^2} + \frac{A_2}{\lambda^4} + \frac{A_3}{\lambda^6} \quad (1)$$

where A_i (i = 0,1,2,3) are the Cauchy's dispersion parameters and λ is the wavelength in nm.

The statistical parameter used to define how well the measured data fit the Cauchy's dispersion equation is the adjusted coefficient of determination, $R^2_{adj.}$

2.5 Abbe number

To further compare dispersions of the liquids analyzed, Abbe numbers were calculated for D, F and C spectral lines, according to the formula [2]:

$$\text{Abbe Number} V_D = \frac{n_D - 1}{n_F - n_C} \quad (2)$$

Where n_D, n_F and n_C are the refractive indices of the material at 589.3, 486.1 and 656.3 nm respectively.

2.6 Intensity along the optical axis

A 1 mM solution of the dye Rhodamine b was dissolved 10% v/v into each of the mounting media tested in this work, and mounted in slides. 70 μm Z-stacks were captured with a 63X 1.4 NA oil immersion objective, with a 1 μm separation between optical sections.

2.7 Spectra

The absorption and emission spectra were measured with a Cytation 5 spectrophotometer (Biotek, Vermont, U.S.A.): suspensions of fluorophores in TDP, TDE, VS, Dako and PBS were measured within single wells of a black-walled, clear-bottom 96-well microplate (Corning Incorporated, NY, U.S.A.). Alexa Fluor phalloidin probes were used at a concentration of 2.6 μM and DAPI at 11.4 mM. The volume used in each measurement is 100 μL.

2.8 Cell culture, transfection and immunocytochemistry

HeLa (ATCC, clone CCL-2) and HEK293 cells were grown in DMEM and SH-SY5Y in DMEM-F12, supplemented with 10% fetal bovine serum and antibiotics at 37°C in 5% CO_2.

For the imaging experiments, cells were seeded on glass coverslips. When grown to a confluency of about 80%, they were fixed in 4% formaldehyde. The cells were subsequently permeabilized with 0.1% Triton-X 100, washed in PBS, then incubated in blocking buffer composed of 10% bovine serum, 0.05% Triton X-100 in PBS for 30 minutes and incubated with the primary antibody (polyclonal anti pan-tubulin, ATN02, Cytoskeleton). After

Biomedical Optics EXPRESS

overnight incubation at 4°C, the cells were washed 3 times with PBS for 10 min and incubated with the secondary antibody (Alexa Fluor 488, A-11015, Thermo Fisher Scientific) for 1.5 h. Nucleus staining was performed by incubating cells in the presence of 3 μM DAPI for 10 min (62248, Thermo Fisher Scientific). Actin cytoskeleton was stained by incubating for 20 minutes in 130 nM Alexa Fluor phalloidin or 100 nM SiR-actin.

Biological markers used are: anti-tubulin polyclonal primary antibody (sheep host) (Cytoskeleton, No. ATN02), monkey anti sheep secondary antibody conjugated to Alexa FluorTM 488 (Themo Fisher Scientific, No. A-11015), DAPI (Thermo Fisher Scientific, No 62248) and Alexa Fluor488 phalloidin (Thermo Fisher Scientific, No A12379), Alexa Fluor 647 phalloidin (Thermo Fisher Scientific, No A22287) and Alexa Fluor 568 phalloidin (Thermo Fisher Scientific, No A12380) and SiR-actin (Cytoskeleton, CY-SC001).

For fluorescent protein expression, HeLa cells were seeded on glass coverslips and transfected after 24 hours using lipofectamine 2000 (Thermo Fisher Scientific, No 11668019) with either pAC γactin EGFP or pAC ßactin mCherry. Transfection was performed according to the protocol of the manufacturer.

2.9 Mounting procedure and imaging

Fixed samples prepared for microscopy were incubated in different dilutions of aTDP to facilitate the exchange of water and mounting medium as described in [3]. The three dilutions were prepared with 10, 25 or 50% of aTDP, 25% PBS and water. Incubation time for each solution was 10 minutes. Two final incubations were performed in aTDP before the final mounting in aTDP. Mounting in VectaShield and Prolong Diamond was performed according to the respective technical data sheet.

A LSM-710-NLO confocal microscope (Zeiss, Germany) equipped with a LCI Plan-Neofluar 25x/0.8 Imm Korr DIC M27 and an alpha Plan-Apochromat 63x/1.46 Oil Korr M27 immersion objectives were used for imaging. For phase contrast experiments an AXXIO Observer.A1 microscope, with 10X/0.25 NA was used.

2.10 Cell size analysis

Twenty micrographs of HEK293 cells stained with fluorescent phalloidins and DAPI were included in the analysis, 4 mounted in PLD, 7 mounted in aTDP and 9 mounted in PBS. Independent binarization of the 2 channels was performed estimating thresholds by Otsu's algorithm [4]. Once the binarized images were obtained, a morphological closure operation using monostructural elements was applied [4]. The number of cells in a micrograph was determined by the number of nuclei; when apparently joint nuclei were detected, a k-means clustering analysis was used to solve the nuclei division. The regional average size of the cells was calculated dividing the surface filled with actin by the number of nuclei counted in the region. The whole image analysis was performed using Matlab (MathWorks).

2.11 Mixtures of TDP-TDE

Three mixtures containing aTDE and aTDP at different concentrations were also tested as mounting media: solution M1 contains 25% aTDP, solution M2 contains 50% and solution M3 is made of 75% aTDP. For the mounting process, the same procedure as in the case of aTDP was followed: cells were incubated in solutions of 10, 25 and 50% concentration of mixture in PBS before mounting.

3. Results

3.1 Refractive index

The refractive indices of TDP and TDE at increasing concentrations in water were measured. The experimental set of data obtained corresponds to n_D and is shown in Fig. 1, where the linear relation found between refractive index and concentration in water is reported.

Biomedical Optics EXPRESS

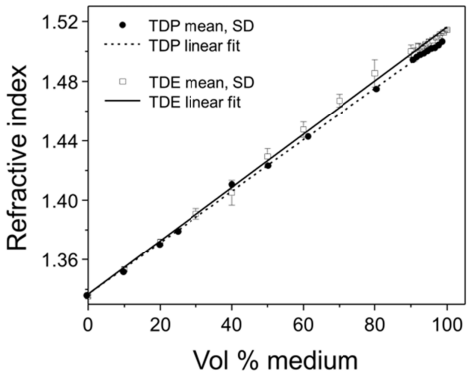

Fig. 1. The refractive indices of TDP and TDE at different concentrations in water are described by a linear relation.

The refractive index of diluted TDP and TDE can be tuned to any value from 1.33 to 1.508 for TDP and to 1.515 for TDE.

3.2 Dispersion measurements and curve fitting

For the measurement of dispersion, a drop of each liquid analyzed was assessed with a refractometer, using 10 discrete regions of the visible spectrum. Regardless of the light source used (LED or laser), a monochromator was employed to set a fixed spectral width for all the measurements so that each light source was quasi-monochromatic. A correction for the glass prisms dispersion was performed as in [5,6].

The averaged experimental points are plotted in Fig. 2, together with the Cauchy fitting described by the dispersion equation with 4 terms. The Cauchy approximation gives good results when used in the visible range [7], hence it was selected for its ease of use; on the other hand, the data were fitted also with the Sellmeier distribution, which resulted in a comparable outcome (data not shown).

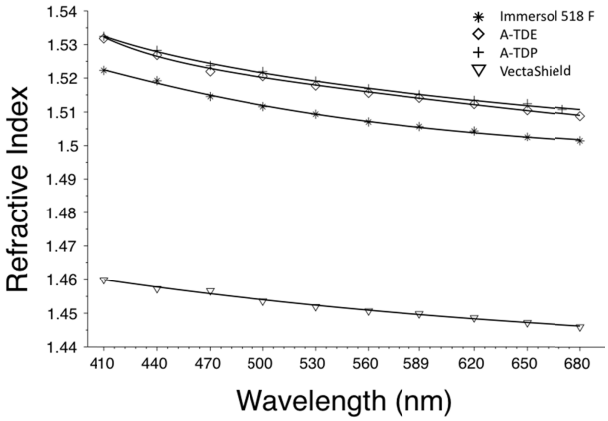

Fig. 2. Experimental data points and Cauchy fitting for the dispersion curve of aTDP, aTDE, the commercial mounting medium Vectashield and the immersion liquid Immersol 518 F.

The fitting parameters are shown in Table 1, together with the corresponding R^2_{adj}. These values vary between 0.986 and 0.995, which shows a good fitting of the curve to the experimental values. All the curves show normal dispersion and the refractive index dependences on the wavelength display similar behavior.

Biomedical Optics EXPRESS

Table 1. Constants of Cauchy formula of TDP, TDE, Vectashield and Immersol 518 F at a temperature of 21 °C.

Parameter (nm)	Immersion oil	aTDE	aTDP	Vectashield
A_0	1.49043	1.478040	1.49254	1.43294
A_1 (nm)	12199.9	21517.70	2781.66	7424.59
A_2 (nm^2)	–15773E + 05	–4.0651E + 09	8.29063E + 08	–6.48647E + 08
A_3 (nm^4)	1.2075E + 14	3.317730E + 14	–7.49276E + 13	2.80746E + 13
R^2	0.98939441	0.9952367	0.994396958	0.986122463

For immersion oil, five n reported in the technical datasheet of the product (Immersionsoele, 2004 [8]) were compared to the values obtained with our system, at corresponding wavelengths: the average difference of the two series of n is 0.00020, with the maximum variation being 0.00044, which shows good agreement between the two sets of data (see Data File 1).

For the commercial medium VectaShield, the only refractive index available from the literature was the one corresponding to 590 nm [9]: the value that can be interpolated from our model (1.449) corresponds to the published value (1.45).

TDE was presented as mounting medium by Staudt et al. and some points of its dispersion curve were reported graphically in the original paper [3]. In our work, we have analyzed the dispersion behavior in a larger spectral region and, as for the other media, we have calculated the mathematical approximation that allows to interpolate the refractive index in any given point of the visible spectrum.

In the case of the new medium TDP, the only n information previously available, to our knowledge, was the value given by the producer, $n_D^{20} = 1.51$; the value we measured is 1.5056, again in good agreement.

3.3 Abbe number

The constringence or Abbe number (Eq. (2)) of the liquids analyzed, which measures the variation of the refractive index with the wavelength, shows that the substance with the highest V_D among those analyzed in this work is VectaShield (57.35), while aTDP (46.17) and aTDE (45.88) show dispersion similar to that of immersion oil (46.07) (Table 2).

Table 2. Dispersion of TDP, TDE, Vectashield and Immersol 518 F (Abbe numbers)

Media	n_D	n_F	n_C	Abbe number
aTDP	1.5056	1.5134	1.5025	46.17
aTDE	1.5142	1.5214	1.5102	45.88
Vectashield	1.4496	1.4549	1.4470	57.35
Oil immersion	1.5152	1.5230	1.5119	46.07

3.4 Effects of n mismatch on confocal image stacks

We have measured the fluorescent intensity along the optical axis in slides where the dye Rhodamine b was diluted and mounted in the different mounting media used. As expected, the mounting media with higher n are those that better perform in this test (Fig. 3).

Biomedical Optics EXPRESS

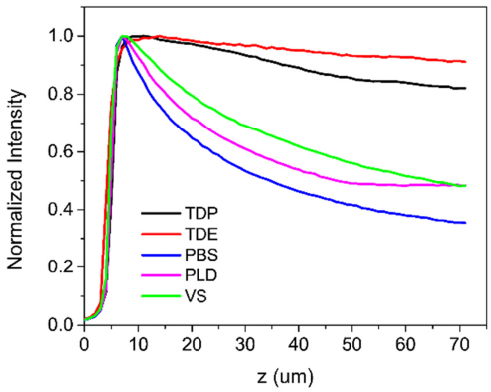

Fig. 3. Fluorescent intensity decay along the z axis for the mounting media tested in this work.

TDP, which displays slightly lower refractive index compared to TDE, shows a slightly more pronounced intensity drop in Z (7% for TDP versus 4% for TDE at 35 µm), although not comparable with commercial mounting media and water-based PBS, which shows the most rapid loss of intensity (50% at 35 µm). In confocal systems, the rapid decay of fluorescent intensity along the Z axis has been shown to be caused by aberrations induced by the n mismatch between the coverslip and the mounting medium [1].

3.5 Spectra

For the three dyes, as expected, the absorption and emission spectra are altered by the solvents. The normalized spectra for DAPI, Alexa Fluor 488 and Alexa Fluor 647 are shown in Fig. 4. The three dyes solvated with TDP experienced a red shift when compared to their spectral behavior in PBS. The shift in the absorption spectra peak position of DAPI and Alexa Fluor 488 is less than 19 nm and there is no shift of emission spectra in both cases. The shift of the absorption spectrum of Alexa Fluor 647 is around 15 nm and the shift for emission spectrum is 25 nm. In five out of six cases, the three dyes display larger emission shifts in the commercial mounting media used in the work. The absorption spectrum of Alexa Fluor 647 in VS was barely detectable under the same conditions.

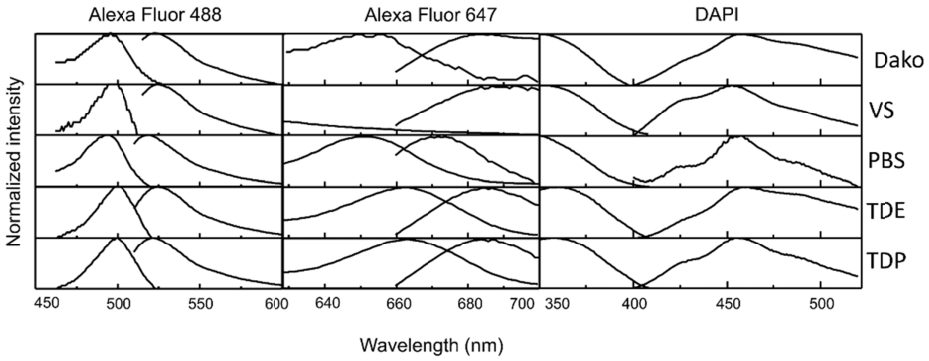

Fig. 4. Solvatochromism of DAPI, AlexaFluor 488 and AlexaFluor 647 dissolved in the media used in this work. A red shift is observed in the absorption and emission spectra of the three different dyes in TDP, as well as in the other mounting media, compared to spectra in PBS.

In order to compare effective fluorescence behavior of the dyes in TDP and PBS, the ratio $QY_{relTDP} = \frac{Abs_{PBS}}{Abs_{TDP}} \bullet \frac{Em_{TDP}}{Em_{PBS}}$ was calculated for the three dyes used [3]. Quantum yields relative

Biomedical Optics EXPRESS

to TDP are higher for both DAPI and Alexa Fluor 647: the QY_{relTDP} is 1.934 for DAPI and 1.57 for Alexa Fluor 647, indicating for both stronger fluorescence in TDP compared to PBS. For Alexa Fluor 488 QY_{relTDP} is 0.36, which indicates weaker fluorescence in TDP compared to PBS.

3.6 Cells mounted in PLD, aTDE and aTDP

In order to test if TDP was a suitable mounting medium for cells labeled with fluorescent phalloidins, HeLa cells stained with Alexa Fluor 647 phalloidin and mounted in either PLD, 97% aTDE or aTDP were imaged.

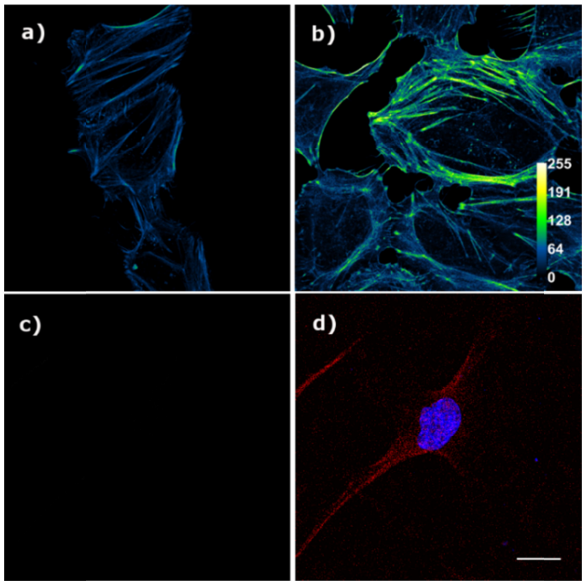

Fig. 5. Actin cytoskeleton of HeLa cells labeled with Alexa Fluor 647 phalloidin and mounted a) in PLD, b) aTDP and c) aTDE. Identical acquisition parameters were used for images a, b and c, while laser power was reduced from 3% to 2.4% in panel b to avoid saturation. Panel d is a post processed merge of the DAPI channel and the AlexaFluor 647 image of panel c with increased brightness and contrast. Scale bar 20 µm.

In cells mounted in aTDP or ProLong Diamond the typical actin cytoskeleton structure is visible thanks to the properly contrasted fluorescent staining (Figs. 5(a) and 5(b)) while in cells mounted in 97% aTDE, it is not possible to detect the fluorescence coming from actin fibers or any other structure (Figs. 5(c)-5(d)). TDP is therefore a chemical with high similarity to TDE, both in its structure and in optical properties, but its use as a mounting medium is compatible with phalloidin-based staining of actin structures in cells.

After demonstrating its compatibility with the phalloidin staining, its performance with other labeling mechanisms and fluorophores was then tested. Six common probes were tested with TDP: phalloidins conjugated to the Alexa Fluor 488, 568 and 647 dyes, rhodamine conjugated to jasplakinolide, DAPI and Alexa Fluor 488 conjugated to a secondary antibody for the recognition of an antitubulin Ig. On the other hand, the selected cell lines HEK293, HeLa and SH-SY5Y allowed us to test the mounting medium with a variety of filamentous actin organizations.

In HEK 293 cells actin filaments are organized mostly in a meshwork and lamellipodia; thus, the AF 488 phalloidin signal is concentrated in those structures (Fig. 6(a)). In HeLa cells the actin cytoskeleton presents thick and dense stress fibers that are involved in cell attachment to some substrates (Fig. 6(b)). In SH-SY5Y cells the filamentous actin is concentrated on the extremes of those polarized cells, in the region that corresponds to the

Biomedical Optics EXPRESS

pseudo-dendrites and axon of this neuronal line (Fig. 6(c)). The cytoskeleton of cells mounted in TDP is well preserved and fluorescence of the probes persists in actin filaments: the toxin phalloidin and its conjugated fluorophores decorate the actin filaments with no evidence of destabilization.

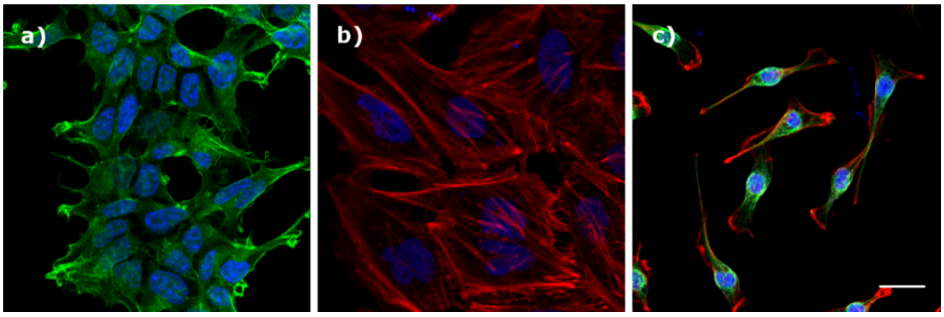

Fig. 6. Micrographs of 3 cell lines labeled with different fluorescent phalloidins and DAPI, mounted in aTDP. a) HEK293 cells stained with Alexa Fluor 488 phalloidin, b) HeLa cells stained with Alexa Fluor 568 phalloidin and c) Sh-sy5y cells stained with Alexa Fluor 647 phalloidin. Scale bar 20 µm.

The DAPI staining is properly localized in the nuclei of the cells, without background signal caused by any undesired displacement of the dye induced by the presence of TDP. In SH-SY5Y cells the architecture of the tubulin cytoskeleton, revealed with indirect staining with fluorophore-carrying antibodies, is not affected after mounting in TDP.

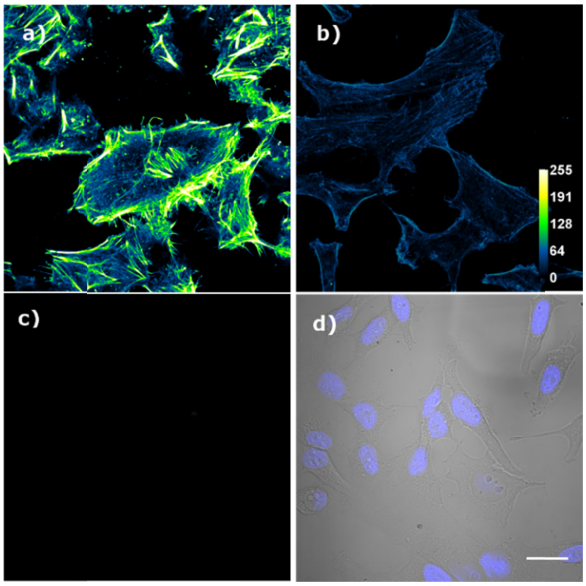

Fig. 7. SiR-actin stained HeLa cells, mounted in a) VS, b) aTDP and c) aTDE. Panel d is a merge of bright field and DAPI staining corresponding to the picture in panel c. Identical acquisition parameters were used for images a, b and c. Scale bar 20 µm.

HeLa cells labeled with SiR-actin and mounted in PLD, aTDP and 97% aTDE are shown in Figs. 7(a), 7(b) and 7(c) respectively. For cells mounted in the commercial mounting medium and in aTDP, morphology is well preserved and the fluorescence allows to appreciate the structural details, while in 97% aTDE no fluorescence or distinguishable morphology of actin filaments is appreciated, suggesting that a similar phenomenon occurs when TDE is used for mounting toxin-marked actin filaments, phenomenon which is not observed when substituting with TDP.

Biomedical Optics EXPRESS

The behavior of TDP was also studied with genetically encoded fluorescent actin. Two plasmids were transfected to obtain fluorescent actin, fused either with a red-emitting protein (mCherry) or green-emitting (EGFP). Figure 8 qualitatively shows that the fluorescent features of the actin cytoskeleton of transfected HeLa cells are independent of the mounting medium used or the spectral variant of the fluorescent protein expressed.

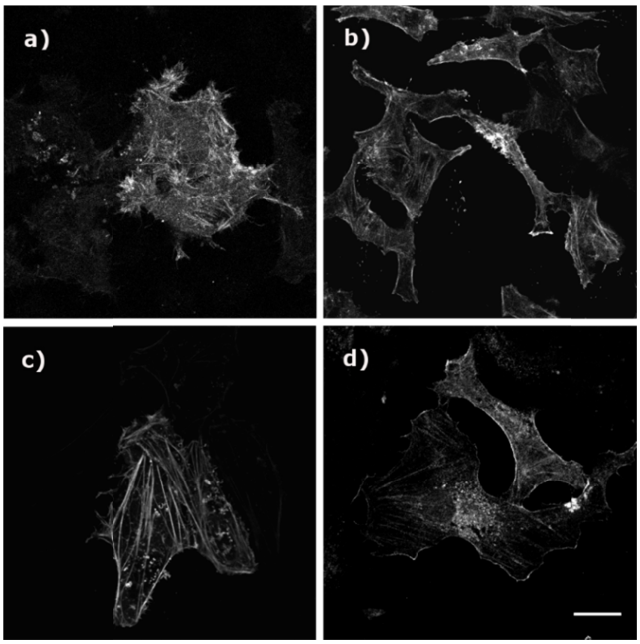

Fig. 8. HeLa cells transfected with: pAC actin mCherry and mounted in a) VS and b) aTDP. HeLa cells transfected with γactin EGFP mounted in c) VS and d) aTDP. Scale bar 20 µm.

3.7 Cell size analysis

Cell slides were prepared using aTDP, ProLong Diamond and PBS as mounting media for fluorescence microscopy. As TDP is a viscous medium, some cell shrinking could happen if the mounting procedure is not performed in a stepwise manner. In order to estimate whether there was a difference in the size of cells mounted in aTDP compared to cells mounted in the commercial mounting medium and in PBS, images of HEK293 cells labeled with fluorescent phalloidins and DAPI were analyzed. The average size of cells mounted in PLD resulted in 384.9 μm^2 vs 388.4 μm^2 in aTDP and 370 μm^2 in PBS. No cell shrinking is thus observable after mounting in aTDP, confirming that the use of this mounting medium doesn't induce manifest morphological changes in the cells. Figure 9 shows the histograms of the regional average cell size in the three mounting media.

Biomedical Optics EXPRESS

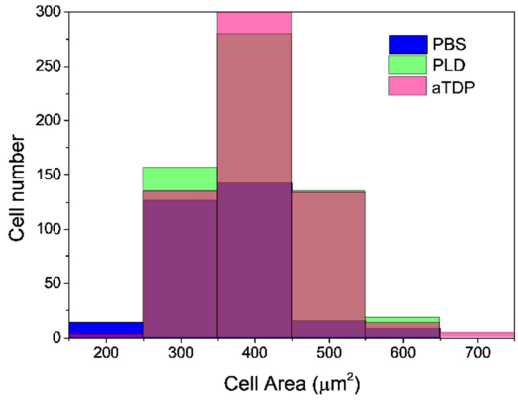

Fig. 9. Distribution of regional average sizes of cells mounted in PBS, PLD and aTDP, in blue, green and pink, respectively. The regions where the three overlap are shown in purple, while light brown indicates overlap between PLD and aTDP bars.

3.8 Mixtures

The three solutions M1, M2, M3 prepared by mixing aTDE and aTDP were used as mounting medium for HeLa cells previously stained for filamentous actin with Alexa Fluor 488 phalloidin. Images from cells mounted in M1, M2 and M3 differ in the fluorescence intensity of labeled actin structures. In cells mounted in M1, few and very thin stress fibers could be observed and the fluorescence intensity is low (Fig. 10(a)). The cells mounted in M2 display higher fluorescence and the actin filaments observed are thicker than those of cells mounted in M1 (Fig. 10(b)). In contrast, the distribution of filamentous actin in cells mounted in M3 is consistent with that of HeLa cells mounted in a commercial mounting medium, with thick and dense stress fibers, and the fluorescence intensity is higher than that of the cells mounted in M1 and M2 (Fig. 10(c)).

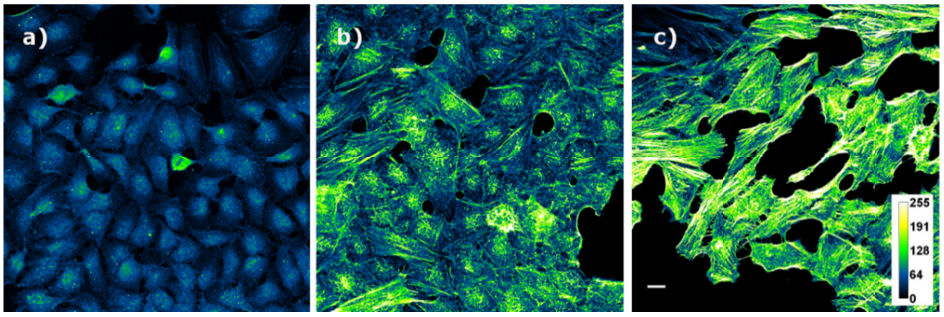

Fig. 10. HeLa cells stained with Alexa Fluor 488 phalloidin and mounted in a) M1, b) M2 and c) M3. Scale bar 20 μm. Identical acquisition parameters were used for the three images, while laser power was reduced from 2% to 1.8% in panel c to avoid saturation.

The refractive index of M1, M2, M3 and also of aTDE and aTDP were measured to verify that the n of a mounting medium based on TDP could be increased by adding TDE. A linear relation between the proportion of aTDE in the mix and refractive index is shown in Fig. 11 (n_{aTDE} = 1.5156, n_{M1} = 1.5123, n_{M2} = 1.5104, n_{M3} = 1.5077, n_{aTDP} = 1.5052).

Biomedical Optics EXPRESS

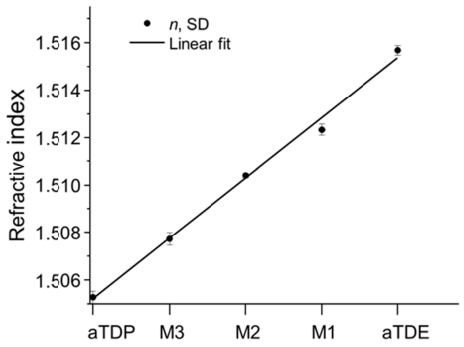

Fig. 11. Variation of refractive index of the mixtures according to the relative composition in aTDE and aTDP.

Therefore, not only the presence of TDP in the mixtures reduced the destabilization of the phalloidin staining produced by TDE, but also the refractive index could be better adjusted to that of immersion oil.

4. Discussion

TDP comprises many desirable characteristics in a mounting medium: it is a colorless, non-toxic liquid, miscible in water and with a high refractive index. Those features could be exploited to achieve high resolution and three-dimensional reconstruction of biological samples. TDP´s optical characteristics are suitable for high resolution fluorescence microscopy of multi-stained samples, with the additional benefit of being compatible with the most common molecule used for labeling filamentous actin in fixed cells, phalloidin [10]. The particular interest on its compatibility with the staining based on phalloidin arises from the fact that the chemically related, high resolution mounting medium TDE could not be used when employing this toxin [3]. Interestingly, both phalloidin and jasplakinolide, two toxin-based actin labeling compounds, are compatible with the use of TDP but are destabilized in presence of TDE.

Immunostaining is the alternative for decoration of actin filaments when fluorophore-conjugated toxins are not a possibility. Still, phalloidin staining has many advantages over immunostaining: phalloidin binds specifically to filamentous actin reducing the background signal from globular actin observed in immunostained samples [11], besides requiring fewer, faster steps in the staining protocol and providing more defined images compared to the punctuated appearance of microfilaments stained with antibodies.

We tested the applicability of TDP with popular dyes used to stain specific structures in three different cell lines. The dyes were selected according to their spectra and labelling mechanism: DAPI binds strongly and selectively to the A-T rich regions of DNA, also increasing its blue fluorescence upon binding [12]; Alexa Fluor dyes as well as rhodamine are fluorescent probes that could be conjugated to targeting molecules, conferring them fluorescence. In our work, Alexa Fluor dyes were bound to secondary antibodies and to phalloidin, while silicon rhodamine was bound to jasplakinolide. The use of different targeting molecules allowed us to test the performance of TDP as mounting medium when a fluorescent molecule binds directly to its target (i.e. DAPI), when a fluorophore is introduced via the specific non-covalent interactions mediated by antibodies (Alexa Fluor 488 decoration of microtubules) and when the fluorophores are carried by toxins (filamentous actin labeling). The Alexa Fluor dyes used (488, 568 and 647) were selected according to their spectral distribution in order to provide alternatives for multicolor staining experiments. HEK293, HeLa and SH-SY5Y cell lines were selected because of their different actin arrays and also

Biomedical Optics EXPRESS

since they differ in cell size and morphology, allowing the imaging and test for performance of our mounting medium with different cytoskeletal architectures. The analysis of samples confirmed that TDP could be used as mounting medium, since the conventional distribution of DAPI, tubulin and filamentous actin staining in epithelial, cervix cancer and neuroblastoma cells was observed. The lack of morphological distortions was also confirmed by our cell size analysis. Additionally, transfected cells mounted in TDP were also imaged, confirming that TDP is compatible also with fluorescent proteins.

Knowing the solvatochromism of probes dissolved in the mounting media is important to determine excitation and detection wavelengths of the fluorescence microscope set up and establish if the excitation sources and filters, as well as the detection filters, are appropriate and efficient for the fluorescence of each experiment. The excitation wavelengths used in this work were those recommended by the fluorophore providers and each fluorophore was imaged using the same excitation and emission parameters in all experimental conditions, i.e. when mounted in PLD, aTDE or aTDP. The bathochromism observed in the spectra of the dyes when TDP is the solvent is subtle, therefore no changes in filters or detectors were necessary. Fluorophore-solvent interactions also have an effect over the fluorophore quantum yield of the dyes used: for Alexa Fluor 647 and DAPI, the relative quantum yield indicates stronger fluorescence brightness when embedded in TDP relative to PBS. In case of Alexa Fluor 488 the brightness is lower, similarly to what happens with Oregon Green 488 as reported in [3]. This might suggest that similar non-covalent molecular interactions take place between “fluorescein-based dyes” and both sulfides media.

A key feature of TDP compared to most commercial media is its refractive index, which by being close to that of immersion oil reduces the refraction caused by the n mismatch and the consequent aberrations in Z. It has been demonstrated that the loss of intensity when imaging deeper into a fluorescent medium, in a confocal system, can be solely explained by aberrations [1]. Spherical aberrations induced by a n mismatch provoke a larger spread of the focus; the spreading of the illumination and detection PSF caused by aberrations affects resolution and intensity [13]. When imaging, the object space, made of the immersion liquid, glass coverslip and the mounting medium-embedded sample, is necessarily heterogeneous. However, differences in the dispersion behavior of the components could led to additional aberrations (i.e. chromatic). Therefore, the selection of the mounting and immersion fluids could be based on the assumption that, for equal conditions of n_D, similar dispersion on the two sides of the coverslip is most desirable, especially when detecting several fluorophores in a Z-stack, as is the case when studying colocalization in a volume [14]. As the homogeneity of n improves the axial resolution, which is critical when imaging deep into thick samples, optical sectioning techniques like confocal, lightsheet and multiphoton microscopy are already benefitting from the use of refractive index matching liquids that enable even deeper imaging [15]. Noteworthy, some index matching liquids were also shown not to interfere with the generation of second harmonics for the stain-free imaging of collagen fibers in the forward direction [16].

Another factor that affects imaging inside 3D samples is unwanted lateral scattering caused by heterogeneities in biological tissues. Clarification, a group of techniques that achieves the downsizing of light deviation by means of chemical reduction of tissue scattering [17], makes extensive use of media with high refractive index, including TDE [18]. It is safe to predict that TDP, due to the chemical similarity to TDE and high n, could be useful for volume fluorescence microscopy, whether this implies clarification or not.

The physico-chemical behavior of mixtures is often unpredictable; for instance, the refractive index of binary mixtures is not always accurately described by mixing rules [19]. For this reason, the effect of mixing aTDE with aTDP on the refractive index of the solution was tested, as well as the performance of the mixtures as mounting media in biological slides. We found that the refractive indices of the mixtures linearly increased with the addition of aTDE making it possible to tune the n from 1.505 to 1.5123. Also, by mixing aTDP and

Biomedical Optics EXPRESS

aTDE in three different proportions we observed dramatic differences on the confocal images, which were tightly dependent on the aTDP:aTDE ratio employed for mounting the slides: on the one hand, the destabilizing effect of TDE on the labeling of actin with fluorescent phalloidins was confirmed; on the other hand, staining loss was hindered by increasing the content of TDP. In other words, by playing with the amount of each medium, we were able to increase the *n* of the mounting medium based on TDP, besides diminishing the destabilizing effect of TDE on the toxin-based actin staining.

Index matching liquids are necessary in microscopy either for imaging into tissue or to achieve the highest possible resolution when required; TDP represents a new, flexible option for these microscopy applications. Additional optical uses of TDP may include optofluidics [20], which combines liquids and photonics, or the related area of tunable optics [21]. Tunable *n* liquids can be also advantageously used in particle image velocimetry, where tunability associated to miscibility in water make TDP a potentially good solvent for both dynamic light scattering, where differences in *n* must be minimized, and diffusing wave spectroscopy, where large differences in *n* are pursued [22,23].

Funding

Consejo de Ciencia y Tecnología del Estado de Guanajuato (SICES number 094/2016CIO); and CONACYT (Mexico, Grant No. 293523, Apoyo al Fortalecimiento de la Infraestructura Científica y Tecnológica 2018).

Acknowledgments

We thank Dr. Y. Barmenkov for lending us the monochromator and letting us use the supercontinuum laser, Dr. E. Morales for the use of Cytation 5 and J.C. Armas and J.E. Landgrave for helpful discussions.

Disclosures

The authors declare that there are no conflicts of interest related to this article.

References

1. S. Hell, G. Reiner, C. Cremer, and E. H. K. Stelzer, "Aberrations in confocal fluorescence microscopy induced by mismatches in refractive index," J. Microsc. **169**(3), 391–405 (1993).
2. H. (Heinrich) Hovestadt, J. D. (J. D. Everett, and A. Everett, *Jena Glass and Its Scientific and Industrial Applications* (London, New York, Macmillan, 1902).
3. T. Staudt, M. C. Lang, R. Medda, J. Engelhardt, and S. W. Hell, "2,2′-thiodiethanol: a new water soluble mounting medium for high resolution optical microscopy," Microsc. Res. Tech. **70**(1), 1–9 (2007).
4. R. C. Gonzalez and R. E. Woods, *Digital Image Processing (3rd Edition)* (Prentice-Hall, Inc., 2006).
5. J. Rheims, J. Köser, and T. Wriedt, "Refractive-index measurements in the near-IR using an Abbe refractometer," Meas. Sci. Technol. **8**(6), 601–605 (1997).
6. S. Kedenburg, M. Vieweg, T. Gissibl, and H. Giessen, "Linear refractive index and absorption measurements of nonlinear optical liquids in the visible and near-infrared spectral region," Opt. Mater. Express, OME **2**, 1588–1611 (2012).
7. A. Samoc, "Dispersion of refractive properties of solvents: Chloroform, toluene, benzene, and carbon disulfide in ultraviolet, visible, and near-infrared," J. Appl. Phys. **94**(9), 6167–6174 (2003).
8. "immersionsoele.pdf," (n.d.).
9. N. Olivier, D. Keller, V. S. Rajan, P. Gönczy, and S. Manley, "Simple buffers for 3D STORM microscopy," Biomed. Opt. Express **4**(6), 885–899 (2013).
10. J. Small, K. Rottner, P. Hahne, and K. I. Anderson, "Visualising the actin cytoskeleton," Microsc. Res. Tech. **47**(1), 3–17 (1999).
11. E. M. De La Cruz and T. D. Pollard, "Transient kinetic analysis of rhodamine phalloidin binding to actin filaments," Biochemistry **33**(48), 14387–14392 (1994).
12. M. Kubista, B. Akerman, and B. Nordén, "Characterization of interaction between DNA and 4′,6-diamidino-2-phenylindole by optical spectroscopy," Biochemistry **26**(14), 4545–4553 (1987).
13. J. Pawley, ed., *Handbook of Biological Confocal Microscopy*, 3rd ed. (Springer US, 2006).
14. G. C. Sieck, C. B. Mantilla, and Y. S. Prakash, "Volume measurements in confocal microscopy," Methods Enzymol. **307**, 296–315 (1999).
15. C. Fouquet, J.-F. Gilles, N. Heck, M. Dos Santos, R. Schwartzmann, V. Cannaya, M.-P. Morel, R. S. Davidson,

Biomedical Optics EXPRESS

A. Trembleau, and S. Bolte, "Improving Axial Resolution in Confocal Microscopy with New High Refractive Index Mounting Media," PLoS One **10**(3), e0121096 (2015).
16. T. A. Theodossiou, C. Thrasivoulou, C. Ekwobi, and D. L. Becker, "Second Harmonic Generation Confocal Microscopy of Collagen Type I from Rat Tendon Cryosections," Biophys. J. **91**(12), 4665–4677 (2006).
17. D. S. Richardson and J. W. Lichtman, "Clarifying Tissue Clearing," Cell **162**(2), 246–257 (2015).
18. M.-T. Ke, Y. Nakai, S. Fujimoto, R. Takayama, S. Yoshida, T. S. Kitajima, M. Sato, and T. Imai, "Super-Resolution Mapping of Neuronal Circuitry With an Index-Optimized Clearing Agent," Cell Reports **14**(11), 2718–2732 (2016).
19. A. Z. Tasic, B. D. Djordjevic, D. K. Grozdanic, and N. Radojkovic, "Use of mixing rules in predicting refractive indexes and specific refractivities for some binary liquid mixtures," J. Chem. Eng. Data **37**(3), 310–313 (1992).
20. D. Psaltis, S. R. Quake, and C. Yang, "Developing optofluidic technology through the fusion of microfluidics and optics," Nature **442**(7101), 381–386 (2006).
21. S. Sun, W. Yang, C. Zhang, J. Jing, Y. Gao, X. Yu, Q. Song, and S. Xiao, "Real-Time Tunable Colors from Microfluidic Reconfigurable All-Dielectric Metasurfaces," ACS Nano **12**(3), 2151–2159 (2018).
22. Z. Wei, Y. Knapp, and V. Deplano, "Low hazard refractive index and density-matched fluid for quantitative imaging of concentrated suspensions of particles," Exp. Fluids **57**(5), 68 (2016).
23. R. Saksena, K. T. Christensen, and A. J. Pearlstein, "Surrogate immiscible liquid pairs with refractive indexes matchable over a wide range of density and viscosity ratios," Phys. Fluids **27**(8), 087103 (2015).